Hindawi
Advances in Polymer Technology
Volume 2020, Article ID 5456707, 11 pages
https://doi.org/10.1155/2020/5456707

Research Article

Design and Construction of Ag@MOFs Immobilized PVDF Ultrafiltration Membranes with Anti-bacterial and Antifouling Properties

Wentao Xu,[1] **Huaqiang Zhuang**,[1] **Zehai Xu**,[2] **Mianli Huang**,[1] **Shangchan Gao**,[3] **Qingbiao Li**,[4] **and Guoliang Zhang**[1,2]

[1]*College of Chemical Engineering and Materials Science, Quanzhou Normal University, Quanzhou 362000, China*
[2]*Institute of Oceanic and Environmental Chemical Engineering, State Key Lab Breeding Base of Green Chemical Synthesis Technology, Zhejiang University of Technology, Hangzhou 310014, China*
[3]*Key Laboratory of Green Energy and Environment Catalysis, Ningde Normal University, Ningde 352100, China*
[4]*College of Food and Biological Engineering, Jimei University, Xiamen 361021, China*

Correspondence should be addressed to Wentao Xu; xuwentao93@aliyun.com and Guoliang Zhang; guoliangz001@126.com

Received 6 July 2019; Revised 5 September 2019; Accepted 9 September 2019; Published 3 January 2020

Academic Editor: Sébastien Déon

In this work, Ag nanoparticle loading $Mg(C_{10}H_{16}O_4)_2(H_2O)_2$(Ag@MOF) composite material was successfully prepared by a facile strategy, and subsequently Ag-MOFs were used to modify the PVDF ultrafiltration membranes to obtain fouling resistance and higher water flux. The as-prepared PVDF membranes were systematically characterized by a series of analytical techniques such as Water Contact Angle (CA), Scanning Electron Microscopy (SEM), and SEM-mapping. Furthermore, the performance of membranes on antibacterial properties, the pure water flux, and fouling resistance was investigated in detail. Those results showed that the membrane modified by Ag@MOFs containing 30% Ag had the higher anti-bacterial performance, and the clear zone could be increased to 10 mm in comparison with that of blank membrane. Meanwhile, the pure water flux of Ag@MOF membranes increased from 85 L/m^2 h to 157 L/m^2 h, and the maximum membrane flux recovery rate (FRR) of 95.7% was obtained using SA as pollutant, which is attributed to the introduction of Ag@MOF composite material. Based on the above experimental results, it can be found that the Ag-MOF membranes displayed the excellent antibacterial activity, high water flux, and fine fouling resistance. This work provides a facile strategy to fabricate the Ag@MOFs modified membranes, and it shows an excellent anti-bacterial and water flux performance.

1. Introduction

With the growing demand for high water quality, many new technologies of water purification are being developed to supply potable and palatable water to humans. Among these technologies, membrane-based processes have caught tremendous attention with the advantage of their ease of implementation, high efficiency, environment-friendliness, and low cost [1]. Ultrafiltration membranes (UF) have important significance where the pore size is suitable for the treatment of wastewater and ease to recover. PVDF is one of the most common materials used to prepare UF due to its excellent performance such as chemical resistance, good thermal and mechanical properties. However, the inherent hydrophobic nature of PVDF usually gives rise to membrane fouling by interactions between the membrane material and precipitates which include inorganic and organic materials, as well as microbial deposits in the treated water [2]. Membrane fouling results in a decrease in performance of the membrane and limits the use of membranes at longer operating times, including reduction in water flux and solute rejection [3–6].

Hydrophilic surface is supposed to improve the anti-fouling property, and several techniques increase their affinity toward water molecules which have been studied to prepare modified PVDF membranes. Previous works reported that the hydrophilic polymers and Zwitterionic species have been demonstrated as effective and stable modifiers for improving hydrophilicity [7–10]. To improve the immobile of the hydrophilic polymers in membranes, polydopamine (PDA) restoration of aged membrane and segregation-induced in situ

hydrophilic modified membranes have also developed [11, 12]. But these methods are limited by the fact that the hydrophilic modification occurs only on the membrane surface, and washes out of the matrix during membrane formation and operation [13, 14].

In the modification methods, the inorganic nanoparticles have many advantages of high stability and high specific surface area, which was general acceptance to modify the PVDF membrane, such as hollow silica microspheres, ZnO nanoparticles, TiO_2 nanoparticles (NPs) and Fe_3O_4 [15–18]. However, direct modified polymer matrices using simple blending gives rise to a number of deleterious problems, such as aggregation of inorganic nanoparticles into large clusters and leaching from the membrane during operation [19, 20]. The uniform dispersion of nanoparticles in the matrix is also the crucial process for the preparation of organic–inorganic hybrid membranes [21]. Many works have been researched on reconstruction of nanoparticles by the modification with Chemical functionalization and polymerization to prepare UF [22–24].

In the previously reported inorganic materials, AgNPs not only have the character of nanoparticles, such as high efficiency and versatile catalytic reactors for environmental remediation but also gained increasing attention in antimicrobial [25–27]. Due to superb antimicrobial properties of AgNPs, they have become a promising solution of antifouling membranes via blending, dip-coating, anchoring on the membrane surface by cold spray, and grafting with polymerization matrix [28, 29]. The location of AgNPs can decide the diffusivity or release of ionic silver (Ag^+) into membrane matrix, so the location of AgNPs into membrane matrix of the silver nanocomposite with blending method is crucial to obtain antifouling membranes [30]. Like other nanoparticles, due to the high surface energy of AgNPs, it tends to aggregate and makes their antibacterial efficiency diminished if they are simply blended into or coated onto the membrane [31]. To achieve better antibacterial properties, ultrafiltration membranes were prepared with modified AgNPs, such as AgNPs loading MWTNs, Ag-loaded zeolites, and AgNPs embedded with the polymeric spacer or grafted polyethylene glycol (PEG) [32–34]. Previous researches were mainly focused on polymers or inorganic material modified silver nanoparticles. The modified AgNPs with hydrophobic and hydrophilic molecular had seldom been reported, such as MOFs.

MOFs are highly porous and possess remarkable inner surface areas [35, 36]. Due to the varied assortments of structural topologies and diverse applications impending in almost all essential fields like gas capture, membrane separation, chemical sensing, drug delivery, catalyst [37–39]. Recently, MOFs had been used as modifiers in polymer membranes to enhance the mechanical strength and hydrophilic properties of membranes due to its large specific surface area and abundant oxygen-containing surface group, and MOFs had also been added into membrane to prepare antifouling ultrafiltration membranes [40–44]. Their inner channels or pores even can be tailored based on the desired functionality and characteristics of the guest molecules, which make MOFs suitable candidates as delivery systems for encapsulation and controlled release of small vaporous bioactive compounds [45]. AgNPs are assembled on MOF which was deeply researched to prevent bacteria adhesion and growth [46]. Those works provide the possibiligy to fabricate membranes with AgNP modified MOF for solving the problem of scale formation.

In this work, the PVDF/PVP/Ag@MOF (100/3/2) has been used to prepare functional modification of PVDF ultrafiltration membranes using nonsolvent induced phase separation (NIPS). Scanning electron microscopy (SEM), contact angle (CA), X-ray diffraction (XRD), and SEM-mapping were used to characterize the Ag-MOF and membranes. The performances of membranes were investigated using permeability test and the filtration of model protein (BSA) and sodium alginate (SA) solutions. Finally, the anti-bacterial efficiencies of membranes were evaluated by the filter-paper method.

2. Materials and Methods

2.1. Materials. Poly (vinylidene fluoride) (PVDF, FR 904) was provided by Shanghai New Material Co., Ltd. China. Sebacic acid (analytical reagent grade), N,N-dimethyl acetamide (DMAc, analytical reagent grade), polyvinyl pyrrolidone (PVP K-30), Magnesium nitrate hexahydrate (analytical reagent grade), and sodium hydroxide (analytical reagent grade), Ethanol (analytical reagent grade) were all purchased from Sinopharm Chemical Reagent Co., Ltd. China. Silver nitrate ($AgNO_3$, analytical reagent grade), bovine serum albumin (BSA, for molecular biology), Sodium alginate (SA, for molecular biology), beef extract (biological reagent), sodium chloride (analytical reagent grade), glucose (analytical reagent grade), yeast extract (biological reagent), anhydrous sodium dihydrogen phosphate (analytical reagent grade), Nutrient agar and glutaraldehyde (analytical reagent grade) were purchased from Energy Chemical Co., Ltd. China. And *Staphylococcus aureus* (*S. aureus*) was purchased from Guangdong culture collection center. All reagents were used without any further purification. Deionized water was used during the whole experiment.

2.2. Synthesis of MOF. $Mg(C_{10}H_{16}O_4)_2(H_2O)_2$ (Mg-MOF) was obtained using the method described in detail [46], 1.58 g Sebacic acid were adjusted to pH 8.0 with 1 mol/L NaOH solution, then $Mg(NO_3)_2{\cdot}6H_2O$ was added and continuously stirred at room temperature for 1 h. The compound was transferred to autoclave with PTFE lining, and maintained at 15 °C for 72 h. After that, the supernatant fluid was centrifuged and cleaned three times with ethanol and water. Then the prepared samples were dried in a vacuum oven at 150°C, 60°C for 24 h before any characterization tests, and further use.

2.3. Preparation of Ag@MOF. 1 g Mg-MOF was added into 50 mL ethanol, and stirred continuously at 10 min. then, 0.1 mol/L $AgNO_3$ was dropped into the solution and stirred for 1 h at room temperature. After that, the supernatant fluid was reacted with sodium hypophosphite for 24 h at room temperature in the dark. Finally, the solution was treated three times by centrifugation. Then the prepared sample was dried in a vacuum oven at 60°C for 24 h and to further use.

2.4. Preparation of Ultrafiltration Membranes. The PVDF ultrafiltration membranes were fabricated through nonsolvent induced phase separation (NIPS) described in detail [47]. The casting solutions were prepared as follows: The cast solution contained 16.5 wt% PVDF, 0.5 wt% PVP and 83 wt% DMAc. First, the cast solution was vigorously stirred for 12 h at 60°C, and then the casting solutions were degassed at room temperature for at least 24 h to remove air bubbles. The solutions were cast uniformly onto a glass substrate by means of a hand-casting knife with the thickness of 150 μm, and then immersed in a bath filled with deionized water. The formed membranes were kept in distilled water for at least 24 h, and this allows the water soluble components in the membrane to be leached out, which named M0. For the Ag@MOF modified membranes prepared like M0, and 2% Ag@MOFs with the weight ratio of Ag and MOF which are 10%, 20%, and 30% were added excess, named M10, M20, M30.

2.5. Characterization of Ag@MOFs. The crystal structure of the Mg-MOF and Ag@MOFs were characterized by X-ray diffraction (XRD) performed on an X'Pert Pro diffractometer (PANalytical, The Netherlands). Characterization was conducted with copper Kradiation source at a scan rate of 2° per min ranging from 5° to 60°. The structure of the Mg-MOF and Ag-MOF was also characterized by SEM using Quanta F250 scanning electron microscope.

2.6. Characterization of Ag@MOF Modified Ultrafiltration Membranes. Samples of the membranes were sputtered with gold, which were viewed with the microscope at 20 kV. The structure of the membranes was inspected by SEM using Quanta F250 scanning electron microscope. Ag distribution of the membranes was detected using SEM-mapping (SEM equipped EDS from EDAX). Water contact angle measurement was performed with a contact angle system (JYW-200B, china) to assess the membrane hydrophilicity. 1 μl of deionized water was carefully dropped on the top surface, and the contact angle between the water and membrane was measured until no further change was observed. To obtain the accurate result, the experiment was repeated five times at random locations for each sample and then the stable result was reported.

2.7. Measurements of Ag@MOF Modified Ultrafiltration Membranes. The porosity of membranes was measured after removing water from membrane. the calculation of ε (%) is defined as follows [48]:

$$\varepsilon\ (\%) = \frac{W_w - W_d}{\rho_w \times A \times \delta} \times 100, \tag{1}$$

where W_w (g) and W_d (g) are the weights of the wet membranes and the dry membranes respectively. ρ_w is the density of water (g cm^{-3}); A is the area of membrane(cm^2); δ is the thickness (cm) of membrane.

The membrane mean pore radius (nm) was tested by Guerout–Elford-Ferry formula. The data including the water viscosity (η, 8.9×10^{-4} Pa s), the volume of permeate pure water per unit time (Q, m^3 s^{-1}), and the operation pressure (ΔP, 0.1 MPa) were utilized. The formula is as follows:

$$r_m = \sqrt{\frac{(2.9 - 1.75\varepsilon) \times 8\eta\delta Q}{\varepsilon \times A \times \Delta P}}. \tag{2}$$

The experimental setup for flux evaluation was similar to those previously reported [15, 16]. The filtration experiment was conducted using a cross-flow filtration system at room temperature, and the effective membrane area (A) is around 8 cm^2. Each membrane was tested three times and at least 1 L feed was used for the filtration and all the filtration experiments were carried out at 0.1 MPa. The volume of the permeated water (V) was collected and flux (J) was calculated until the permeated water volume remained unchanged at the time interval (Δt). The rejection ratio (R) of model pollutant (BSA, pH 7.4, 1 g/L) was prepared to test, the feed concentrations (C_f) and the permeate concentrations (C_p) were obtained by UV spectrophotometer (280 nm, UV-180). The permeation flux (J) and rejection (R) were calculated using the following equation:

$$J = \frac{V}{A\Delta t}, \tag{3}$$

$$R\ (\%) = \left(1 - \frac{C_p}{C_f}\right). \tag{4}$$

To appraise the antifouling ability of modified membranes, BSA, SA, and mixture (0.5 g/L SA and 0.5 g/L BSA) were used as model pollutant to evaluate the antifouling ability through quantitative analysis. Each sample was first compacted by filtering ultrapure water at 0.20 MPa and 25°C for 30 min. Then, the pressure was lowered to 0.10 MPa to measure the flux of ultrapure water (J) until reaching a constant value. Thereafter, BSA (0.5 g/L, pH 7.4) and mixture (0.5 g/L SA and 0.5 g/L BSA) solution was driven to permeate through the membrane at 0.10 MPa for 30 min, then the membrane was refreshed 20 min with ultrapure water. To further study the flux recovery property of this pollution-filtered membrane, the solution reservoir was replaced with ultrapure water and gained the stable flux (J_1) performed for another 60 min at 0.10 MPa. When the SA (0.5 g/L, pH 7.4) was used as model pollutant to evaluate the antifouling ability, three cycles were conducted in accordance with BSA as model pollutant, and gained the stable flux (J_1, J_2, J_3).

To get downtrend of the flux after pollution, three cycles were also conducted in accordance with BSA as model pollutant, and the ultrapure water flux of every cycle was recorded every 10 min for 60 min at 0.10 MPa.

$$\mathrm{FRR} = \frac{J_n}{J} \times 100\%. \tag{5}$$

To investigate the broad spectrum antibacterial behaviors of the modified PVDF membranes, *S. aureus* was used as the testing organism. Before testing, *S. aureus* was cultivated in sterilized Luria–Bertani (LB) broth overnight at 37°C in a shaking incubator. For qualitative evaluation, an LB agar plate was mixed with 0.1 ml LB broth containing 10^5 CFU/mL of *S. aureus*, and the M0, M10, M20, and M30 with a diameter of

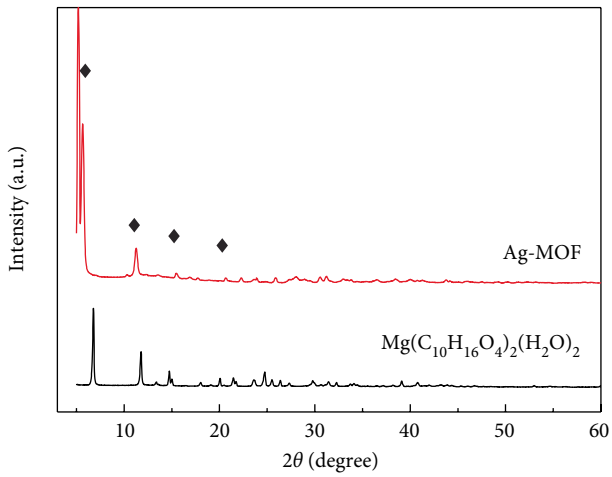

FIGURE 1: Powder X-ray diffraction profiles of simulated.

6 mm were placed on the LB agar plate, then, the LB agar plate was incubated 24 h at 37°C. The antibacterial activity was studied and measured by a clear zone of inhibition in the indicator lawn around the membrane.

3. Results and Discussion

3.1. Characterization of $Mg(C_{10}H_{16}O_4)_2(H_2O)_2$ and Ag@MOF. The structure of the Mg-MOF and Ag@MOF was analyzed using XRD for evaluation of crystalline structure. As shown in Figure 1, the Mg-MOF and Ag@MOF exhibit a broad XRD reflection peak around 6°, 11°, 15°, 21°, which could be assigned to the amorphous structures of Mg-MOF [46]. The result of XRD indicated the construction of Mg-MOF has not changed modified by AgNPs. The Ag@MOFs had not observed diffraction peaks at 38.1°, 44.2° attributed crystalline planes of the face-centered cubic (fcc) structured Ag (JCPDS, 04-0783), which might be veiled by Strong XRD peak of Mg-MOF. To confirm the Ag nanoparticles deposited onto the surface of Mg-MOF, the SEM of Mg-MOF and Ag@MOF was presented in Figure 2, it suggested AgNPs were dispersed homogeneously on Mg-MOF. To further learn the distribution of AgNPs on Mg-MOF, the modified membranes were also characterized by SEM Ag-mapping. The SEM Ag-mapping is presented in Figure 3, which also showed AgNPs are formed homogeneously on the surface of Ag-MOF membranes.

3.2. Membrane Morphology. The surface morphologies and cross-sections of pristine PVDF and Ag@MOF modified PVDF membranes are researched by SEM displayed in Figures 4 and 5. After modification, the surfaces of membranes are relatively smooth except the sample of M30, which accumulated on the top surface with some particles. Those results indicate the nanocomposites are uniformly dispersed on the membrane surface. It is apparent that the top surfaces are a little different between the unmodified and modified membranes, the roughness of membrane surface has only changed a little as the loading quantity of Ag increased. However, the aggregation of Ag-MOF can be observed on the M30 membrane surface, so it is worth mentioning that the forming of cracks and an increase in the pore sizes were caused by the loading amount. The cross-sections of the four membranes had the relative asymmetric and highly inhomogeneous structure with a selective thin microporous upper skin on macroporous voids. This structure was mainly due to the high mutual diffusivity of water and DMAc.

The SEM Ag-mapping of the membrane surfaces was used to make further research study equal distribution of loading displayed in Figure 3. SEM measurement not only gave valuable information to confirm that Ag was successfully doped with membrane, but the Ag of the membrane surface is dispersed homogeneous. The EDX Ag-mapping show the amount of the Ag distribution increased when Ag loading varies from 10–30%.

3.3. Membrane Hydrophilicity. Hydrophilic and hydrophobic properties affect absorption of contaminants on the membrane surfaces and in pore walls, which also decide the separation and antifouling properties of separation membranes. Therefore, many works had been proposed to improve the hydrophilicity of PVDF membrane. The surface hydrophilicity of the modified membranes were evaluated by Water contact angle. As presented in Figure 6, the water contact angle of M0, M10, M20 and M30 were 82.8°, 72.9°, 67.1°, and 63.7°, respectively. The hydrophilicity of membranes was improved after mixing with Ag@MOFs, and the contact angle decreased gradually. The results show that Ag@MOF modified PVDF membranes have a better hydrophilic property. Furthermore, the hydrophilicity of membrane is better as the amount of Ag loading increased in Mg-MOF. Therefore, Mg-MOF with high surface area and Ag loading may play an important role in the hydrophilic property of membrane surface and the hydration effect.

3.4. Filtration Performance of Membrane. The filtration performance of membrane has been measured, as shown in Figure 7. The pristine PVDF membrane had the lowest pure water flux (85 $L/m^2 h$). In comparison, the pure water flux of the modified membranes was improved remarkably, and the water flux has reached 157 $L/m^2 h$ from 85 $L/m^2 h$ of pristine membrane with the membrane modified by the 30% Ag loading Mg-MOF. It is possible that Ag@MOF can attract water molecules inside the membrane matrix and promoted them to pass through the membrane, and accordingly enhance the permeability. The BSA retention of membrane was also evaluated, which showed all modified membranes had raised the retention rate, and the BSA rejection rate was a maximum rate reaching as high as 98.6%, compared to 94.3% of the pure PVDF membranes. This phenomenon can be explained by the fact that the increase in small pores are small enough to effectively prevent BSA molecules caused by adding nanoparticles. In conclusion, the Ag@MOF modified membranes gained higher PWF and better BSA rejection than the pure membranes, especially when the Ag loading of Mg-MOF is 30 wt%.

To explore the influence factor of pure water flux and BSA retention of membrane, the porosity (ε (%)) and mean pore radius (r_m) of different membranes was measured as shown in Figure 8. The ε (%) of Ag@MOF -PVDF membranes were

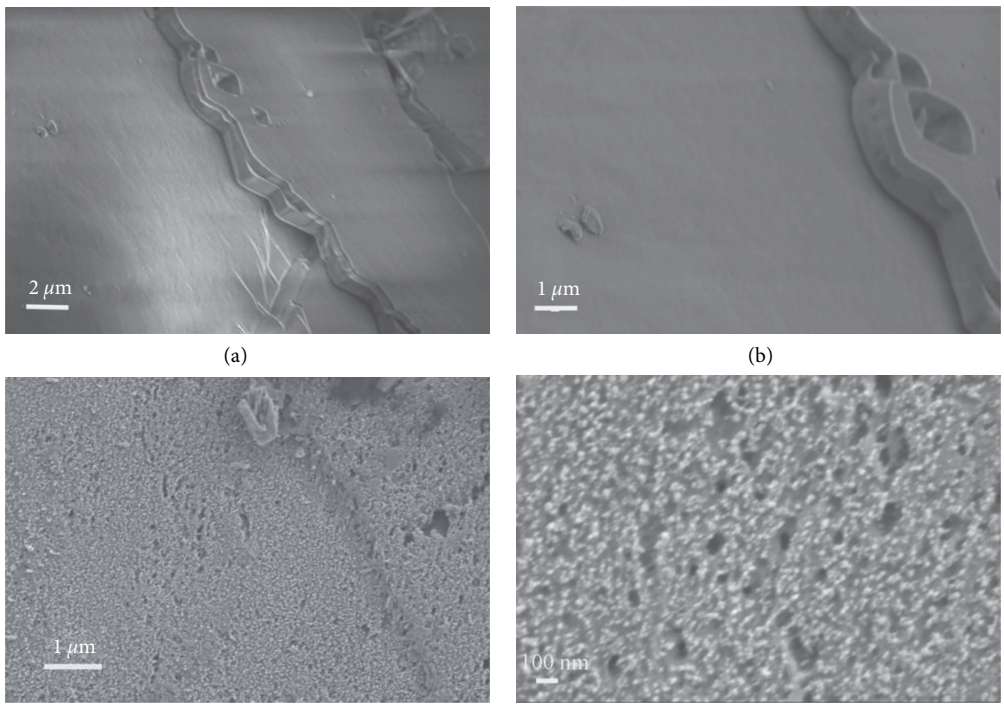

Figure 2: SEM images of the surface of the Mg-MOF (a, b) and Ag@MOF (c, d).

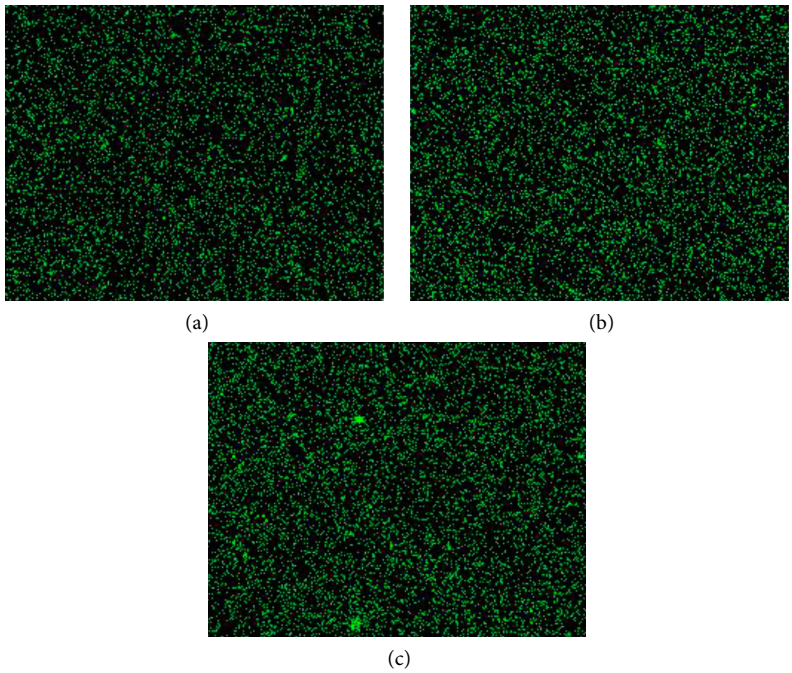

Figure 3: EDX Ag-mapping on the surface of the modified membranes: (a) M10, (b) M20, and (c) M30.

raised as the loading of Ag in the Mg-MOF increased, and the ε (%) reached 30.7 of the M30 from 11.6 of M0. The results explained the flux of the modified membranes increased furthermore. For the mean pore radius (r_m), it was reduced with the increase in the loading of Ag. Compared to 26 nm of the r_m value with M0, the r_m value of M30 was only 20 nm, which is a benefit for the BSA retention of membrane.

3.5. Organic Antifouling Performance of Ag-MOF -PVDF Membrane. Organic antifouling performance learned by the multicycle filtration experiments were first presented with the SA as the colloidal pollutant in Figure 9. The great decline in flux values of all membranes during the first cycle of filtration was displayed, which forms a cake layer on the membrane as the SA with a strong gel. After the first cycle of the fouling test,

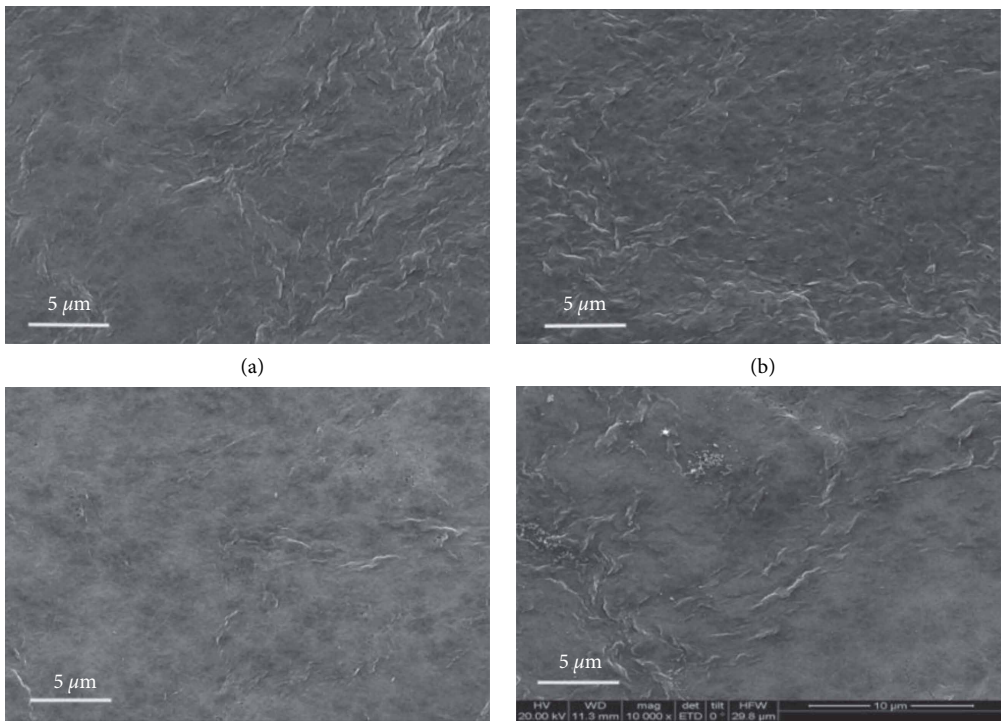

Figure 4: SEM images of the surface of the unmodified and modified membranes: (a) M0, (b) M10, (c) M20, and (d) M30.

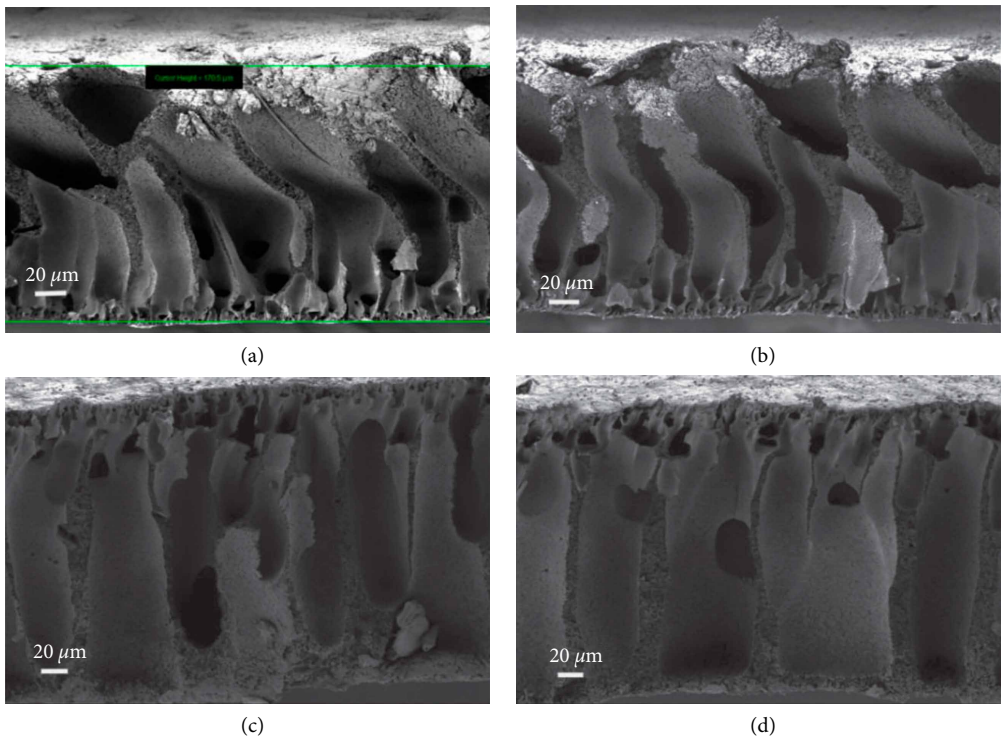

Figure 5: SEM images of the crosssection of the unmodified and modified membranes: (a) M0, (b) M10, (c) M20, and (d) M30.

the result also shows that the modified PVDF membrane have a higher FRR value of 95.7% while the 30% Ag loading Mg-MOF was used as additive, compared to unmodified membrane with only that of 87.5%, which is ascribed to the changes of ionic surface structure. The FRR value of M30 remains above 86% after three cycles of the fouling test, which is the expression of the improved antifouling ability to the cake-layer type fouling formed by SA.

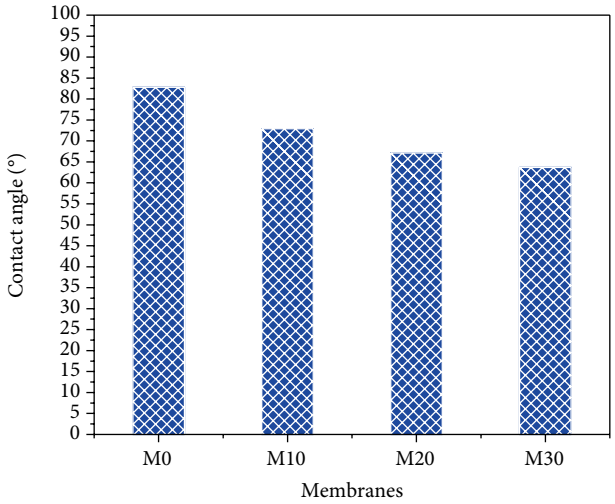

Figure 6: The water contact angle of different membranes surface.

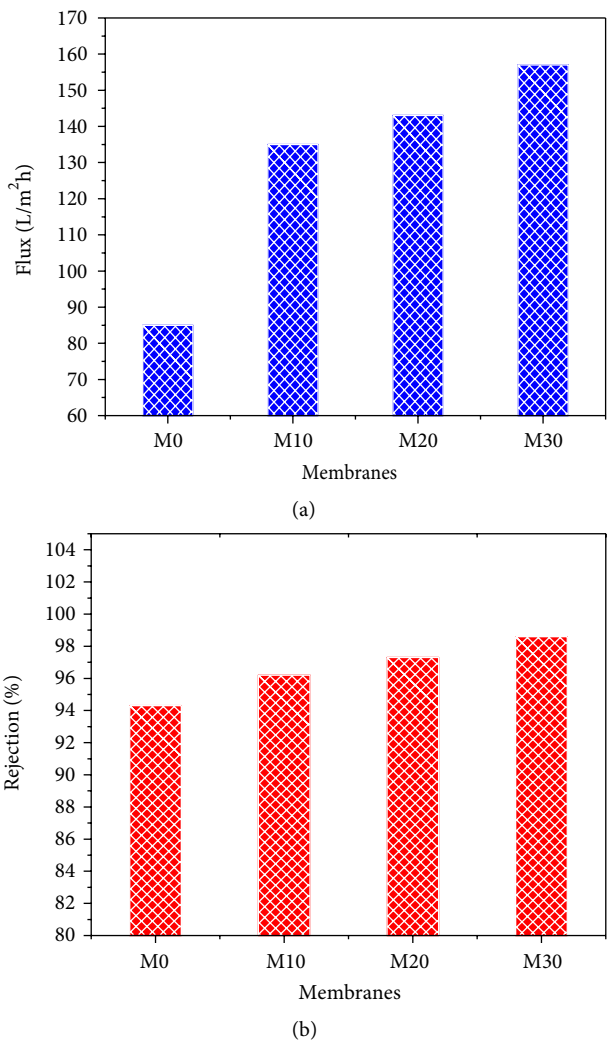

Figure 7: Separation performance of membranes (a) the water flux (b) rejection of BSA using solution containing 200 ppm solute.

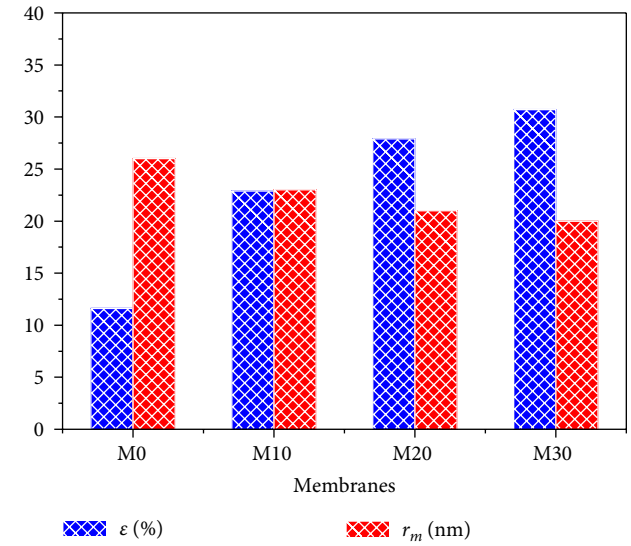

Figure 8: The porosity and mean pore radius of different membranes.

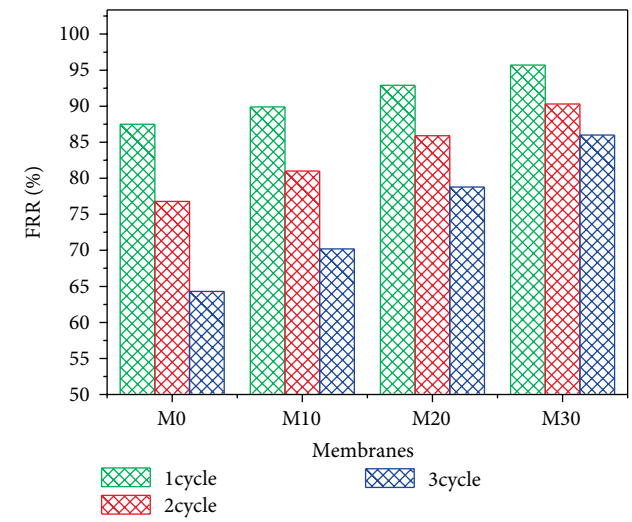

Figure 9: The fouling results of all the PVDF membranes with SA as pollutant.

BSA exhibits strong hydrophobic interactions with the hydrophobic PVDF membrane surface which is also commonly used the pollutant of antifouling ability test. The results show BSA and the mixture of BSA+SA were used to test the antifouling property in Figure 10. The FRR values of the modified PVDF membranes slightly increased in all for BSA, but FRR value reduced as the content of the Ag loading in the MOF increase, and the maximal FRR value reaches 88.5% for M10. The result indicate Mg-MOF may be the reason of raising FRR value of modified membranes, and the reason of reducing FRR value with M30 should be mainly attributable to BSA interact with Ag which caused occlusion of the membrane pores. However, when SA and BSA were provided as the feed solution, the modified membranes have the excellent antifouling effect with the FRR value of 90.4%

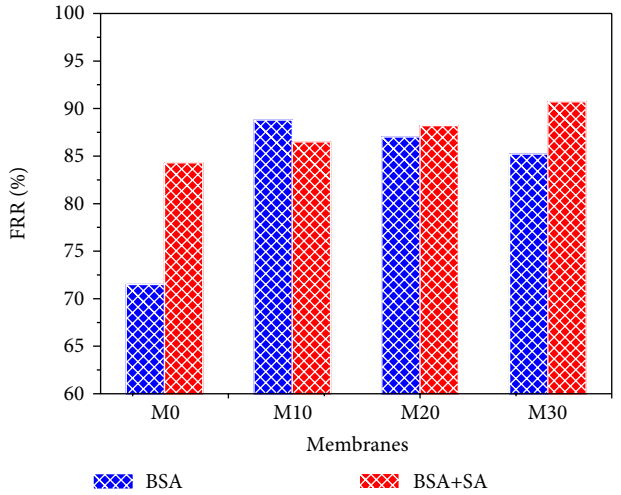

Figure 10: The fouling results of all the PVDF membranes with BSA as pollutant.

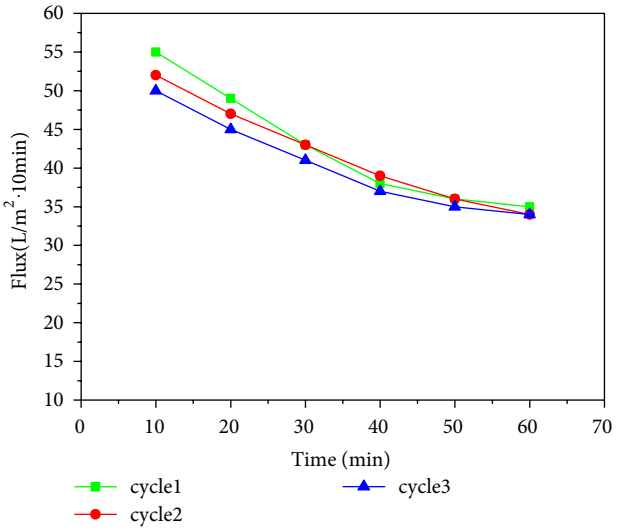

Figure 11: The downtrend of the flux of M30 membranes after pollution with BSA.

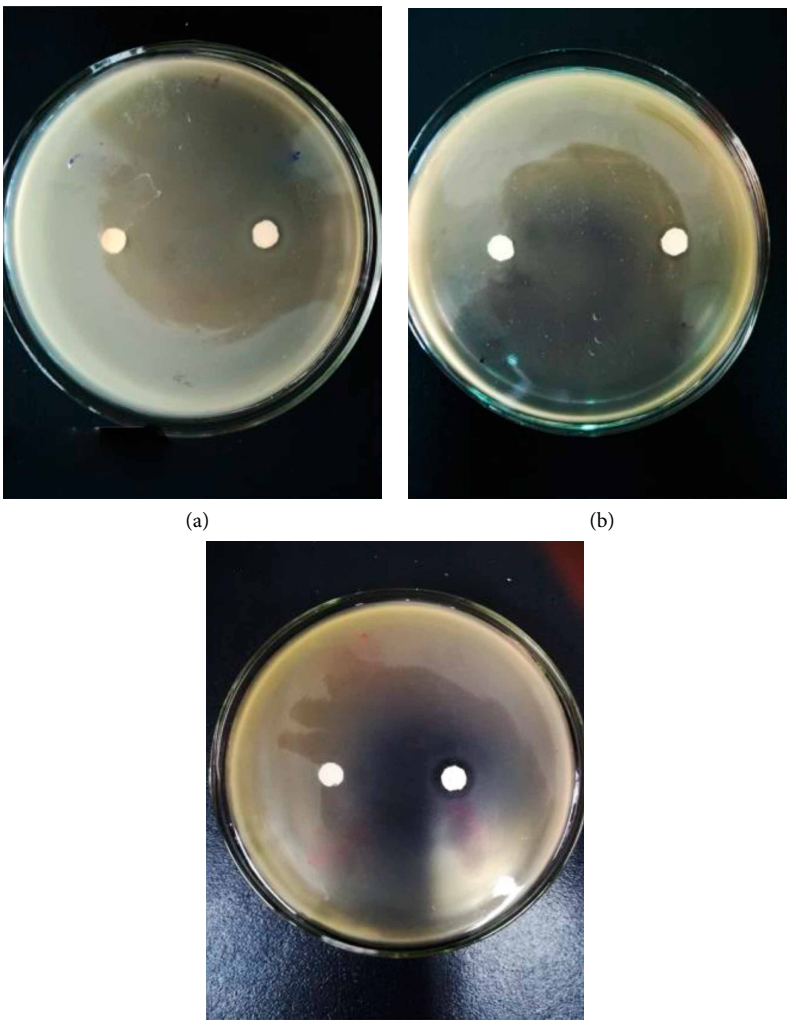

(a) (b)

(c)

Figure 12: Anti-bacterial properties of different membranes (a) M10, (b) M20, and (c) M30.

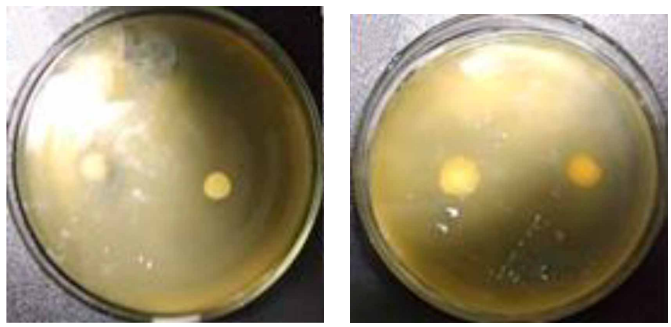

(a) (b)

Figure 13: Anti-bacterial properties of different day with M30 (a) 1 day (b) 3 day.

for M30. It can be inferred that the modified PVDF membranes with an ionic of Ag@MOF were able to exhibit better antifouling ability to the SA contained pollutant feed. This finding should be associated with the cake layer properties of SA itself, which were more easily to form a cake layer on top of the membranes.

To get downtrend of the flux after pollution, three cycles of the flux with M30 were conducted using BSA as model pollutant in Figure 11. The downtrend of the flux declined after pollution for all cycles, and the relative stable flux stage was recorded after working for 40 min. It also showed a little change of the flux was observed among the three cycles, especially for the relative stable flux stage. Those results indicated the modified membrane had better antifouling properties.

3.6. Anti-Bacterial Activity of Membrane. AgNPs had been extensively reported to exhibit various antimicrobial properties. So the anti-bacterial property of membranes was studied in Figure 12. It indicated the zone of inhibition test result of various membranes to *S. aureus*. It could be observed that there is no impact of unmodified membrane to the growth of *S. aureus*. For the M10, M20, and M30, the clear inhibition zones around the virgin membrane were observed, and the inhibition zone increased as the content of Ag. It was identified that the modification of membrane with Ag@MOF containing 30% Ag had highest anti-bacterial, and the clear zone can be increased by around 66% from 6 mm to 10 mm. The results indicated that anti-bacterial property was mainly ascribed to the existence of the silver element on the membrane surface. Although the dissolution rate of the silver metal into Ag^+ ions in these particular conditions were not further learned in this work, the distribution of Ag on the membranes might affect the dissolution rate. The SEM Ag-mapping showed AgNPs are formed homogeneously on the surface of Ag-MOF membranes, which meant the diffusivity or release of ionic silver (Ag^+) into membrane matrix had become easy and might have advantage of the antibacterial activity, as it had reported the location of AgNPs can decide the diffusivity or release of ionic silver (Ag^+) into membrane matrix. . We also further studied the anti-bacterial durability of membranes which were immersed in water showed in Figure 13. The result indicated that the membrane still had anti-bacterial ability after three days, which meant the membrane have better anti-bacterial durability in use [30].

4. Conclusion

The procedure for the fabrication of Ag@MOF-PVDF blended flat sheet membranes had been successfully produced with 3 wt% PVP, 2 wt% Ag@MOF and 100 wt% PVDF in the casting solution. This membrane raised hydrophilicity and water permeation flux of the PVDF membrane. The modified PVDF membrane showed better antibacterial activity and displayed excellent anti-fouling performance. When *S. aureus*. was used as test bacteria, the clear zone could be observed, and the diameter of zone increased by around 66% from 6 mm to 10 mm with M30. The maximum water flux of 157 L/m^2 h was gained using the technology, and The maximum FRR of 95.7% was also obtained in the blend membrane with 30% Ag loading Mg-MOF as additive to measure antifouling ability of pollutant SA, indicating its highest antifouling capacity, which was further supported using the BSA as pollutant. In conclusion, Ag@MOF-PVDF membrane exhibited antimicrobial activity and also enhanced surface hydrophilicity to prevent biofouling during the operation of PVDF membrane.

Data Availability

The [Figure1–Figure 12] data used to support the findings of this study are included within the article.

Conflicts of Interest

The authors declare that they have no conflicts of interest.

Acknowledgments

Thanks for the help of Le Dong (College of Oceanology and Food Science) who provided bacteria and part of equipment. This work was supported by Department of Education, Fujian Province (JAT160417), Fund of Fujian Provincial Key Laboratory of Green Energy and Environment Catalysis (FJ-GEEC201706), The Natural Science Foundation of Fujian Province (2016J01693), Quanzhou Science and Technology Project (grant number 2018C127R).

References

[1] B. P. Tripathi, N. C. Dubey, S. Choudhury, and M. Stamm, "Antifouling and tunable amino functionalized porous membranes for filtration applications," *Journal of Materials Chemistry*, vol. 22, no. 37, pp. 19981–19992, 2012.

[2] P. Le-Clech, V. Chen, and T. A. G. Fane, "Fouling in membrane bioreactors used in wastewater treatment," *Journal of Membrane Science*, vol. 284, no. 1–2, pp. 17–53, 2006.

[3] N. Misdan, A. F. Ismail, and N. Hilal, "Recent advances in the development of (bio)fouling resistant thin film composite membranes for desalination," *Desalination*, vol. 380, pp. 105–111, 2016.

[4] C. Ong, J. Shi, J. Chang et al., "Tannin-inspired robust fabrication of superwettability membranes for highly efficient separation of oil-in-water emulsions and immiscible oil/water mixtures," *Separation and Purification Technology*, vol. 227, p. 115657, 2019.

[5] Y.-H. Zhao, X. Y. Zhu, K.-H. Wee, and R. Bai, "Achieving highly effective non-biofouling performance for polypropylene membranes modified by UV-induced surface graft polymerization of two oppositely charged monomers," *The Journal of Physical Chemistry B*, vol. 114, no. 7, pp. 2422–2429, 2010.

[6] C. Klaysom, B. P. Ladewig, G. Q. M. Lu, and L. Wang, "Preparation and characterization of sulfonated polyethersulfone for cation exchange membranes," *Journal of Membrane Science*, vol. 368, no. 1–2, pp. 48–53, 2011.

[7] J. F. Hester, P. Banerjee, Y. Y. Won, A. Akthakul, M. H. Acar, and A. M. Mayes, "ATRP of amphiphilic graft copolymers based on PVDF and their use as membrane additives," *Macromolecules*, vol. 35, no. 20, pp. 7652–7661, 2002.

[8] C.-H. Zhang, F.-L. Yang, W.-J. Wang, and B. Chen, "Preparation and characterization of Hydrophilic modification of polypropylene non-woven fabric by dip-coating PVA (polyvinyl alcohol)," *Separation and Purification Technology*, vol. 61, no. 3, pp. 276–286, 2008.

[9] S. Boributh, A. Chanachai, and R. Jiraratananon, "Modification of PVDF membrane by chitosan solution for reducing protein fouling," *Journal of Membrane Science*, vol. 342, no. 1–2, pp. 97–104, 2009.

[10] H.-Q. Liang, Q.-Y. Wu, L.-S. Wan, X.-J. Huang, and Z.-K. Xu, "Polar polymer membranes via thermally induced phase separation using a universal crystallizable diluent," *Journal of Membrane Science*, vol. 446, pp. 482–491, 2013.

[11] F. Gao, J. Wang, H. Zhang, H. Jia, Z. Cui, and G. Yang, "Aged PVDF and PSF ultrafiltration membranes restored by functional polydopamine for adjustable pore sizes and fouling control," *Journal of Membrane Science*, vol. 570-571, pp. 156–167, 2019.

[12] H. Sun, X. Yang, Y. Zhang et al., "Segregation-induced in situ hydrophilic modification of poly (vinylidene fluoride) ultrafiltration membranes via sticky poly (ethylene glycol) blending," *Journal of Membrane Science*, vol. 563, pp. 22–30, 2018.

[13] G. Kang and Y. Cao, "Application and modification of poly(vinylidene fluoride) (PVDF) membranes-a review," *Journal of Membrane Science*, vol. 463, pp. 145–165, 2014.

[14] A. Venault, Y.-N. Chou, Y.-H. Wang et al., "A combined polymerization and self-assembling process for the fouling mitigation of PVDF membranes," *Journal of Membrane Science*, vol. 547, pp. 134–145, 2018.

[15] H. Wang, X. Zhao, and C. He, "Innovative permeation and antifouling properties of PVDF ultrafiltration membrane with stepped hollow SiO_2 microspheres in membrane matrix," *Materials Letters*, vol. 182, pp. 376–379, 2016.

[16] S. Liang, K. Xiao, Y. H. Mo, and X. Huang, "A novel ZnO nanoparticle blended polyvinylidene fluoride membrane for anti-irreversible fouling," *Journal of Membrane Science*, vol. 394-395, pp. 184–192, 2012.

[17] H. Younas, H. Bai, J. Shao, Q. Hanc, Y. Ling, and Y. He, "Super-hydrophilic and fouling resistant PVDF ultrafiltration membranes based on a facile prefabricated surface," *Journal of Membrane Science*, vol. 541, pp. 529–540, 2017.

[18] Z. Rahimi, A. A. Zinatizadeh, and S. Zinadini, "Milk processing wastewater treatment in a bioreactor followed by an antifouling O-carboxymethyl chitosan modified Fe_3O_4/PVDF ultrafiltration membrane," *Journal of Industrial and Engineering Chemistry*, vol. 38, pp. 103–112, 2016.

[19] S. Mallakpour and M. Madani, "A review of current coupling agents for modification of metal oxide nanoparticles," *Progress in Organic Coatings*, vol. 86, pp. 194–207, 2015.

[20] R. X. Zhang, L. Braeken, P. Luis, X. L. Wang, and B. V. Bruggen, "Novel binding procedure of TiO_2 nanoparticles to thin film composite membranes via self-polymerized polydopamine," *Journal of Membrane Science*, vol. 437, pp. 179–188, 2013.

[21] F. Liu, N. A. Hashim, Y. Liu, M. R. Moghareh Abed, and K. Li, "Progress in the production and modification of PVDF membranes," *Journal of Membrane Science*, vol. 375, no. 1–2, pp. 1–27, 2011.

[22] L. Zhou, K. Gao, Z. Jiao et al., "Constructing dual-defense mechanisms on membrane surfaces by synergy of PFSA and SiO_2 nanoparticles for persistent antifouling performance," *Applied Surface Science*, vol. 440, pp. 113–124, 2018.

[23] N. Ghaemi, P. Daraei, and S. Palani, "Surface modification of polysulfone membranes using poly(acrylic acid) decorated alumina nanoparticles," *Chemical Engineering & Technology*, vol. 41, no. 2, pp. 261–269, 2018.

[24] Z. Geng, X. Yang, C. Boo et al., "Self-cleaning anti-fouling hybrid ultrafiltration membranes via side chain grafting of poly(aryl ether sulfone) and titanium dioxide," *Journal of Membrane Science*, vol. 529, pp. 1–10, 2017.

[25] L. Rizzello and P. P. Pompa, "Nanosilver-based antibacterial drugs and devices: mechanisms, methodological drawbacks, and guidelines," *Chemical Society Reviews*, vol. 43, no. 5, pp. 1501–1518, 2014.

[26] L. F. Dumée, Z. Yi, B. Tardy et al., "Silver metal nano-matrixes as high efficiency and versatile catalytic reactors for environmental remediation," *Scientific Reports*, vol. 7, p. 45112, 2017.

[27] Z. Yi, S. Zhao, J. Zhang, M. F. She, L. Kong, and L. F. Dumée, "Discrete silver nanoparticle infusion across silica aerogels towards versatile catalytic coatings for 4-nitrophenol reduction," *Materials Chemistry and Physics*, vol. 223, pp. 404–409, 2019.

[28] D. Y. Zhang, Q. Hao, J. Liu et al., "Antifouling polyimide membrane with grafted silver nanoparticles and zwitterion," *Separation and Purification Technology*, vol. 192, pp. 230–239, 2018.

[29] L. F. Dumée, L. He, P. C. King et al., "Towards integrated anti-microbial capabilities: novel bio-fouling resistant membranes by high velocity embedment of silver particles," *Journal of Membrane Science*, vol. 475, pp. 552–561, 2015.

[30] M. Sile-Yuksel, B. Tas, D. Y. Koseoglu-Imer, and I. Koyuncu, "Effect of silver nanoparticle (AgNP) location in nanocomposite membrane matrix fabricated with different polymer type on antibacterial mechanism," *Desalination*, vol. 347, pp. 120–130, 2014.

[31] S. K. Das, M. Motiar, R. Khan et al., "Nano-silica fabricated with silver nanoparticles: antifouling adsorbent for efficient dye removal, effective water disinfection and biofouling control," *Nanoscale*, vol. 5, no. 12, pp. 5549–5560, 2013.

[32] P. Gunawan, C. Guan, X. Song et al., "Hollow fiber membrane decorated with Ag/MWNTs: toward effective water disinfection and biofouling control," *ACS Nano*, vol. 5, no. 12, pp. 10033–10040, 2011.

[33] H. Shi, F. Liu, and L. Xue, "Fabrication and characterization of antibacterial PVDF hollow fibre membrane by doping Ag-loaded zeolites," *Journal of Membrane Science*, vol. 437, pp. 205–215, 2013.

[34] J. A. Prince, S. Bhuvana, K. V. K. Boodhoo, V. Anbharasi, and G. Singh, "Synthesis and characterization of PEG-Ag immobilized PES hollow fiber ultrafiltration membranes with long lasting antifouling properties," *Journal of Membrane Science*, vol. 454, pp. 538–548, 2014.

[35] L. Huang, H. Wang, J. Chen et al., "Synthesis, morphology control, and properties of porous metal-organic coordination polymers," *Microporous and Mesoporous Materials*, vol. 58, no. 2, pp. 105–114, 2003.

[36] U. Mueller, M. Schubert, F. Teich, H. Puetter, K. Schierle-Arndt, and J. Pastré, "Metal–organic frameworks—prospective industrial applications," *Journal of Materials Chemistry*, vol. 16, no. 7, pp. 626–636, 2006.

[37] K. K. Gangu, S. Maddila, S. B. Mukkamala, and S. B. Jonnalagadda, "A review on contemporary metal-organic framework materials," *Inorganica Chimica Acta*, vol. 446, pp. 61–74, 2016.

[38] X. Sun, Q. Xia, Z. Zhao, Y. Li, and Z. Li, "Synthesis and adsorption performance of MIL-101(Cr)/graphite oxide composites with high capacities of n-hexane," *Chemical Engineering Journal*, vol. 239, pp. 226–232, 2014.

[39] C. Wang, X. Liu, N. K. Demir, J. P. Chenbc, and K. Li, "Applications of water stable metal–organic frameworks," *Chemical Society Reviews*, vol. 45, no. 18, pp. 5107–5134, 2016.

[40] J. Ma, X. Guo, Y. Ying, D. Liu, and C. Zhong, "Composite ultrafiltration membrane tailored by MOF@GO with highly improved water purification performance," *Chemical Engineering Journal*, vol. 313, pp. 890–898, 2017.

[41] F. Gholami, S. Zinadini, A. A. Zinatizadeha, and A. R. Abbasi, "TMU-5 metal-organic frameworks (MOFs) as a novel nanofiller for flux increment and fouling mitigation in PES ultrafiltration membrane," *Separation and Purification Technology*, vol. 194, pp. 272–280, 2018.

[42] L. Wang, M. Fang, J. Liu, J. He, J. Li, and J. Lei, "Layer-by-Layer fabrication of high-performance polyamide nanocomposite membrane for nanofiltration applications," *ACS Applied Materials & Interfaces*, vol. 7, no. 43, pp. 24082–24093, 2015.

[43] H. Sun, B. Tang, and P. Wu, "Development of hybrid ultrafiltration membranes with improved water separation properties using modified superhydrophilic metal–organic framework nanoparticles," *ACS Applied Materials & Interfaces*, vol. 9, no. 25, pp. 21473–21484, 2017.

[44] A. Sotto, G. Orcajo, J. M. Arsuaga, G. Calleja, and J. Landaburu-Aguirre, "Preparation and characterization of MOF-PES ultrafiltration membranes," *Journal of Applied Polymer Science*, vol. 132, no. 21, p. 41633, 2015.

[45] J. Vaughn, H. Wu, B. Efremovska et al., "Encapsulated recyclable porous materials: An effective moisture-triggered fragrance release system," *Chemical Communications*, vol. 49, no. 51, pp. 5724–5726, 2013.

[46] A. Mesbah, L. Aranda, J. Steinmetz, E. Rocca, and M. François, "Crystal structure and phase transition of bis-aqua-sebacato magnesium $Mg(C_{10}H_{16}O_4)_2(H_2O)_2$," *Solid State Sciences*, vol. 13, no. 7, pp. 1438–1442, 2011.

[47] X. Li, R. Pang, J. Li et al., "In situ formation of Ag nanoparticles in PVDF ultrafiltration membrane to mitigate organic and bacterial fouling," *Desalination*, vol. 324, pp. 48–56, 2013.

[48] M. A. Mohamed, W. W. Salleh, J. Jaafar et al., "Physicochemical characteristic of regenerated cellulose/N-doped TiO_2 nanocomposite membrane fabricated from recycled newspaper with photocatalytic activity under UV and visible light irradiation," *Chemical Engineering Journal*, vol. 284, pp. 202–215, 2016.